Comparison of Modern Methods for Shock Hydrodynamics

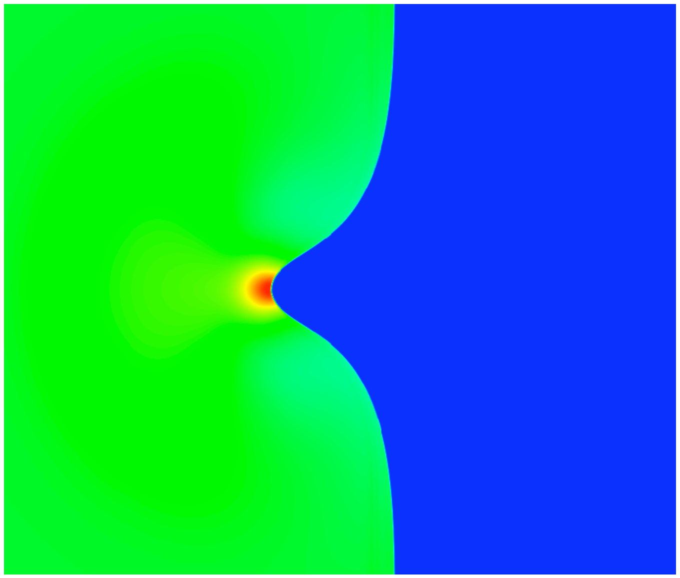

Vienna

June 20–23, 2005

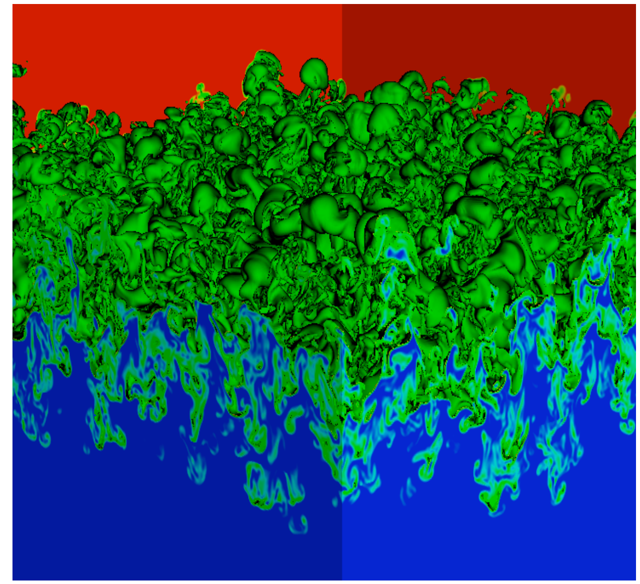

Andrew W. Cook

Lawrence Livermore National Laboratory

Collaborators: Bill Cabot and Jeff Greenough

This work was performed under the auspices of the US Department of Energy by the University of California, Lawrence Livermore National Laboratory under Contract No. W-7405-ENG48.

High-order methods can be used for shock capturing.

- Spectral and 10^{th}-order compact schemes for spatial derivatives
- 4^{th}-order Runge-Kutta timestepping
- Variable-order artificial viscosity
- 8^{th}-order dealiasing filter

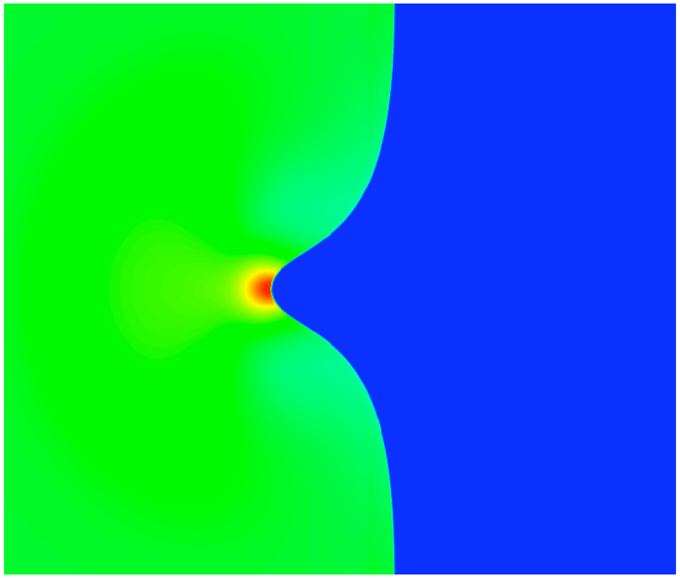

Mach 10 shock on SF6 cylinder

What are the benefits?

The multi-fluid large-eddy equations can be cast in Navier-Stokes form.

$$\dot{\rho}_\alpha + \nabla \cdot \left(\rho_\alpha \boldsymbol{u} - \boldsymbol{J}_\alpha \right) = 0$$ **(species continuity)**

$$\dot{\boldsymbol{m}} + \nabla \cdot \left(\boldsymbol{mu} + p\overleftrightarrow{\delta} - \overleftrightarrow{\boldsymbol{\tau}} \right) = \rho \boldsymbol{g}$$ **(mixture momentum)**

$$\dot{E} + \nabla \cdot \left[E\boldsymbol{u} + \left(p\overleftrightarrow{\delta} - \overleftrightarrow{\boldsymbol{\tau}} \right) \boldsymbol{u} - \boldsymbol{q} \right] = \boldsymbol{m} \cdot \boldsymbol{g}$$ **(mixture energy)**

$$p = \rho (Y_\alpha H_\alpha - e), \quad H_\alpha = \int_{T_0}^{T} c_{p,\alpha}(T')\,dT'$$ **(mixture EOS)**

$$\boldsymbol{J}_\alpha = \rho D_\alpha \nabla Y_\alpha - Y_\alpha \sum_{\alpha=1}^{N} \rho D_\alpha \nabla Y_\alpha$$ **(diffusive mass flux)**

$$\overleftrightarrow{\boldsymbol{\tau}} = \mu \left[\nabla \boldsymbol{u} + (\nabla \boldsymbol{u})^{\mathrm{T}} \right] + \left(\beta - \frac{2}{3}\mu \right) (\nabla \cdot \boldsymbol{u}) \overleftrightarrow{\delta}$$ **(viscous stress)**

$$\boldsymbol{q} = k \nabla T$$ **(conductive heat flux)**

Solution via: 10th-order compact derivatives
4th-order Runge-Kutta timestepping

Hyperviscosity damps high wavenumbers.

$$\mu = \mu_0 + C_\mu \overline{\rho \left| \nabla^r S \right| \Delta^{(r+2)}}, \quad \mathrm{r} = 2,4,6\ldots$$

$$\beta = \beta_0 + C_\beta \overline{\rho \left| \nabla^r S \right| \Delta^{(r+2)}}, \quad \mathrm{r} = 2,4,6\ldots$$

$$S = \left(\overleftrightarrow{S} : \overleftrightarrow{S} \right)^{1/2}, \quad \overleftrightarrow{S} = \frac{1}{2}\left(\nabla \boldsymbol{u} + \boldsymbol{u} \nabla \right)$$

$$\overline{(\ )} = \text{Gaussian filter of width } 4\Delta$$

Increase r for higher formal accuracy.

A dealiasing filter is applied to the conserved variables after each R-K substep.

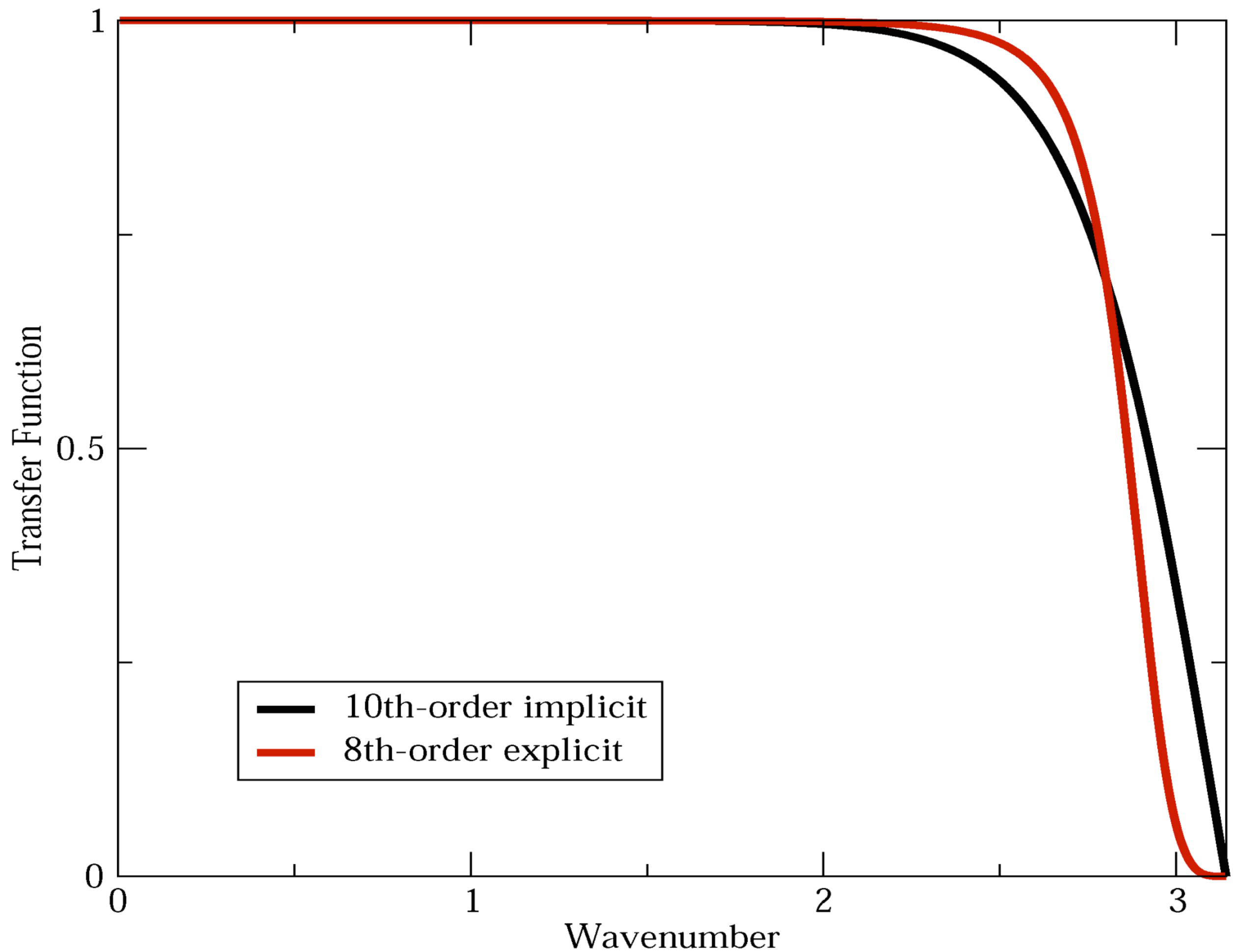

Dealiasing filter preserves functions to 8th order.

Spectral/compact methods capture fine-scale features of Richtmyer-Meshkov instability.

128 ppw | 256 ppw | 512 ppw

Spectral

CENO

M=1.2

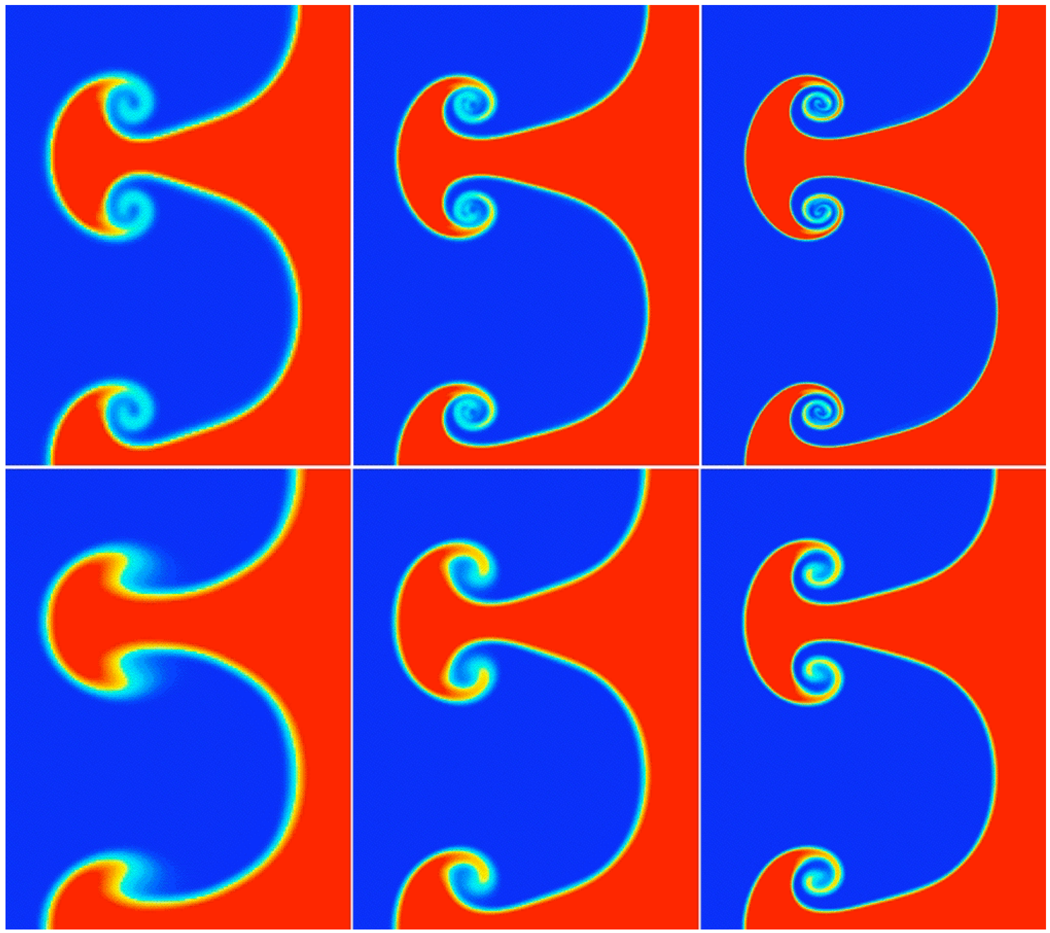

Simulations of Collins-Jacobs air-SF6 experiment

Diffusive schemes can fail for Rayleigh-Taylor instability with very fine-scale perturbations.

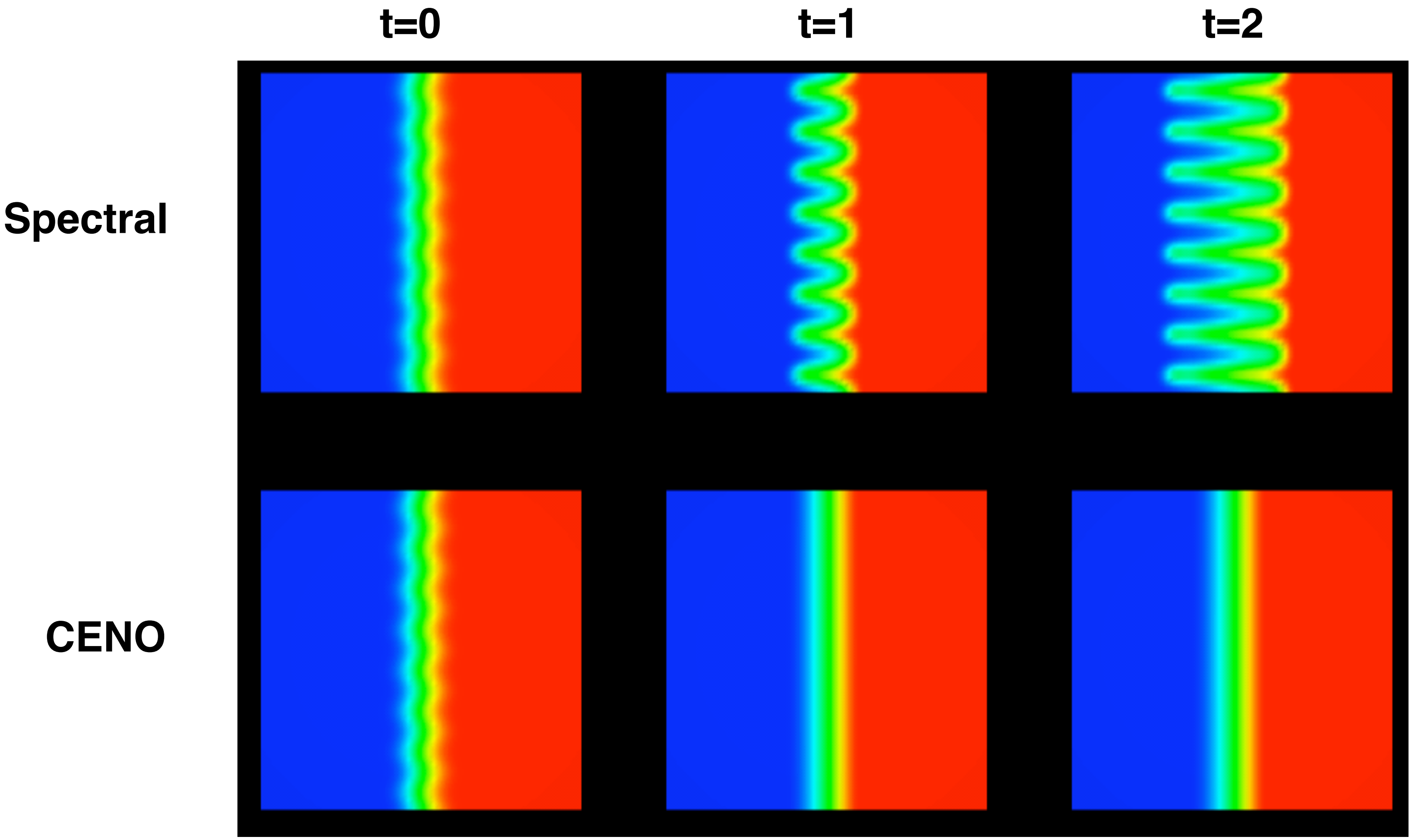

Implicit numerical dissipation wipes out perturbations (8 ppw).

Hyperviscosity remains inactive as long as flow is well resolved.

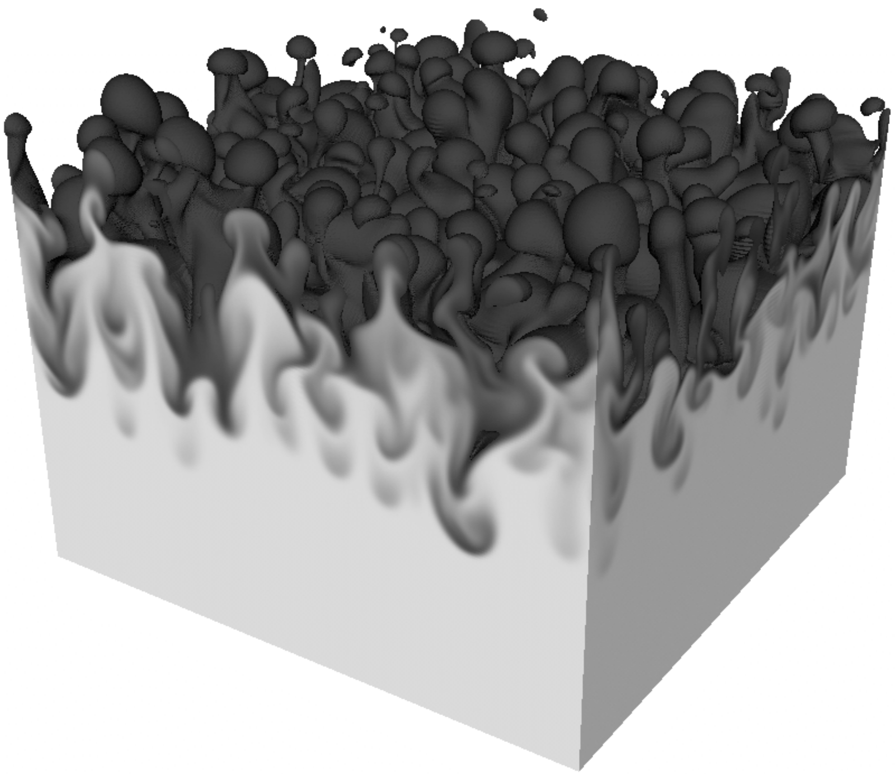

DNS

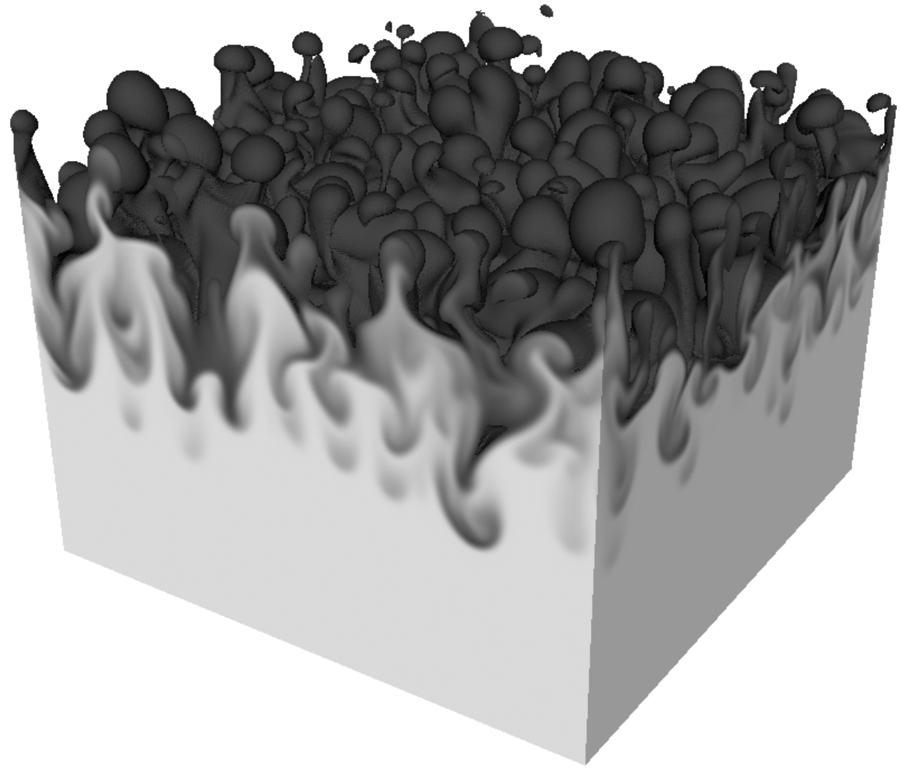

LES

LES → DNS at low Reynolds number

LES continues after DNS runs out of resolution.

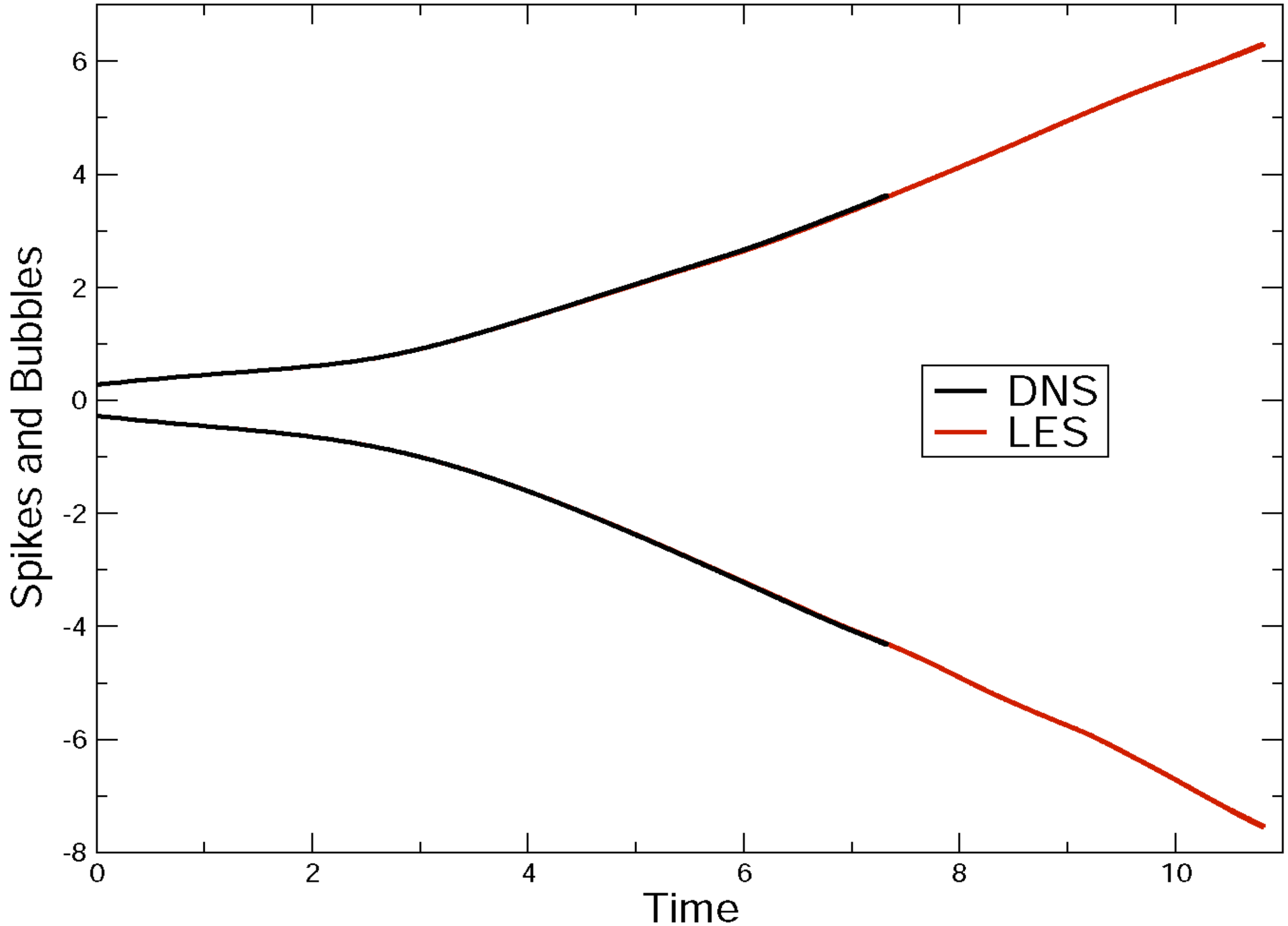

LES extends DNS results to higher Reynolds number.

Hyperviscosity truncates high wavenumbers.

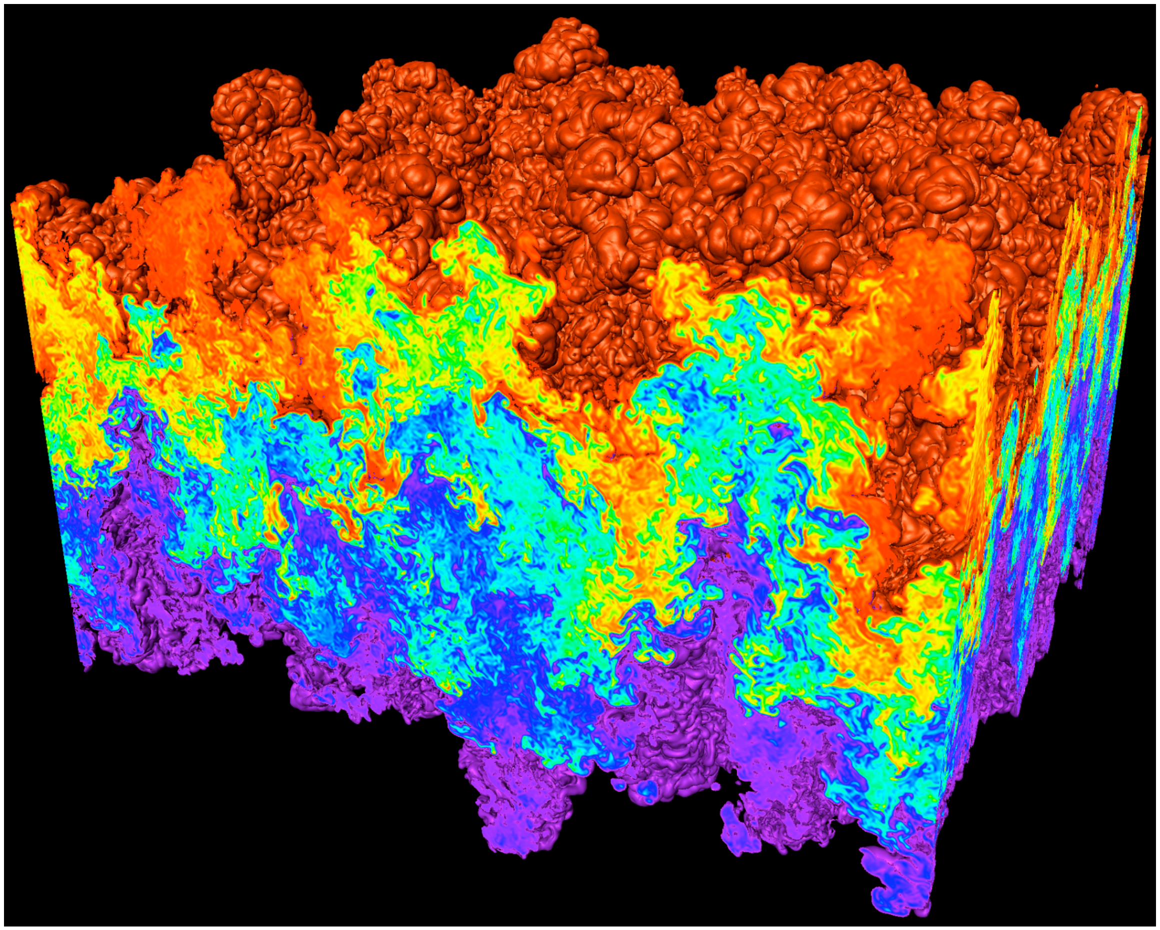

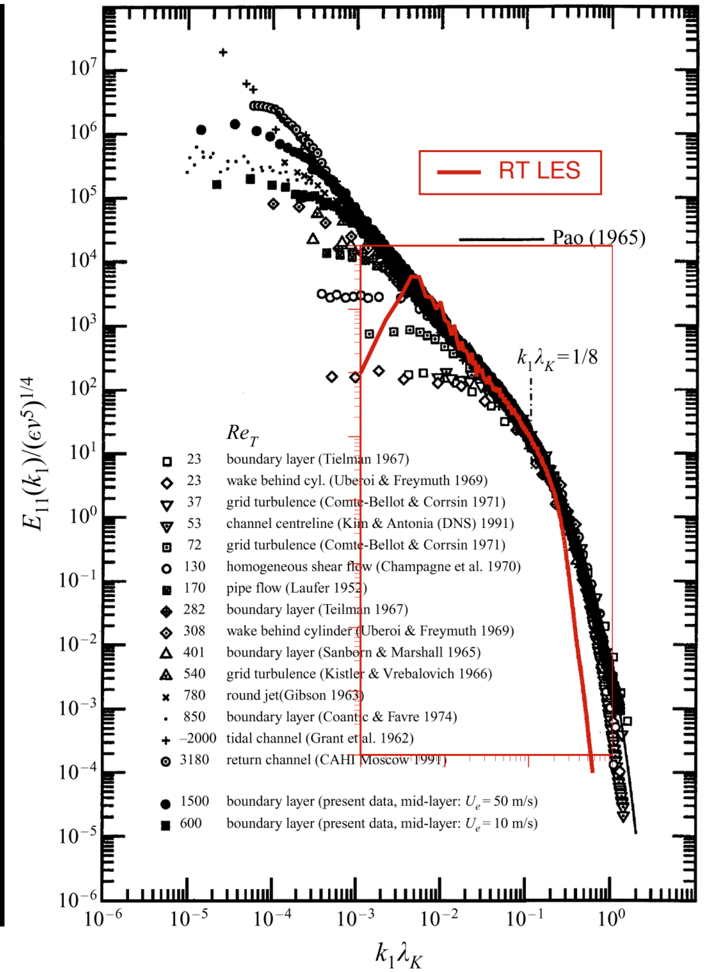

Final Reynolds number > 20,000

Subgrid-scale models reduce Gibbs oscillations.

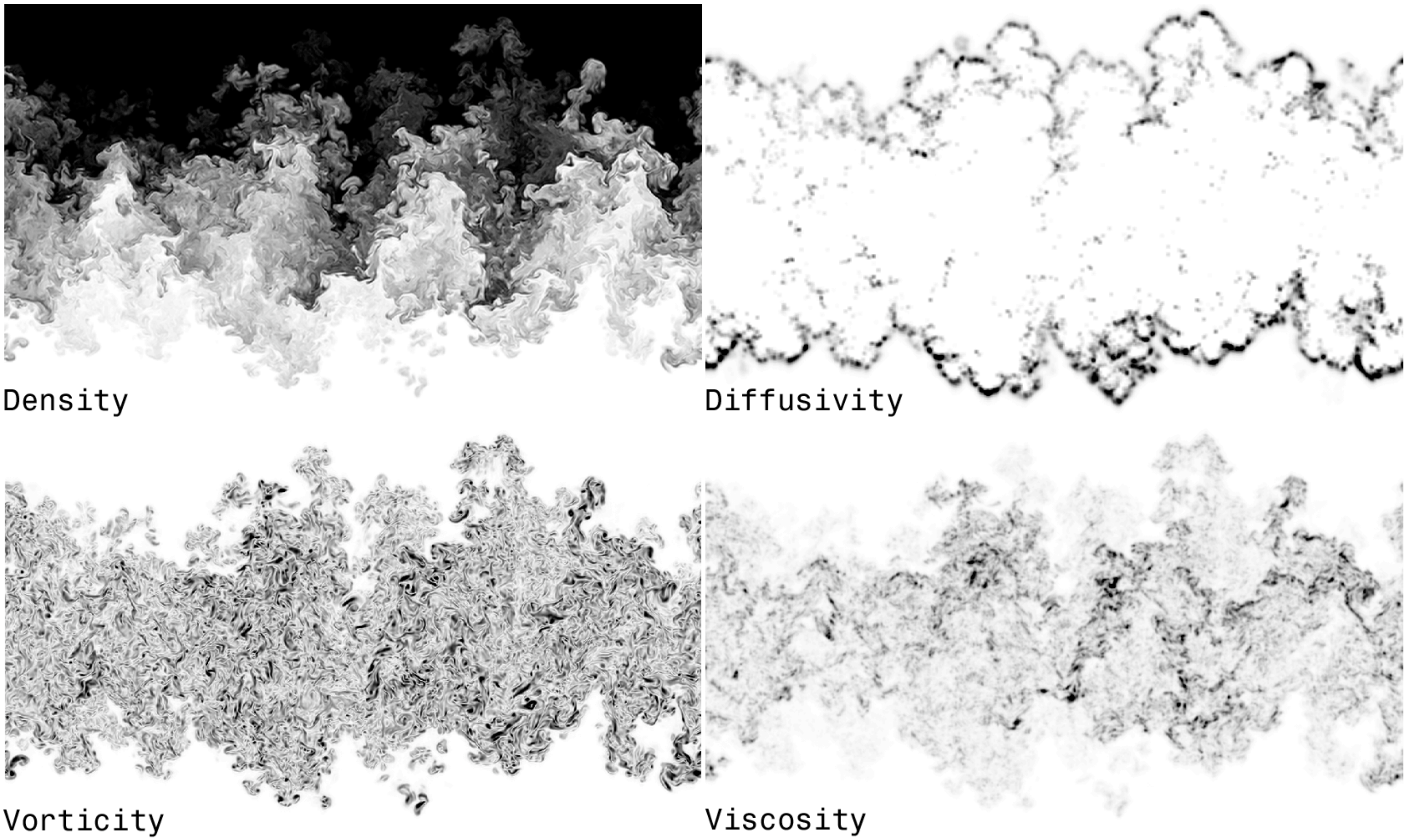

Subgrid-scale viscosity and diffusivity act differently.

A compressible breaking wave provides quantitative code verification.

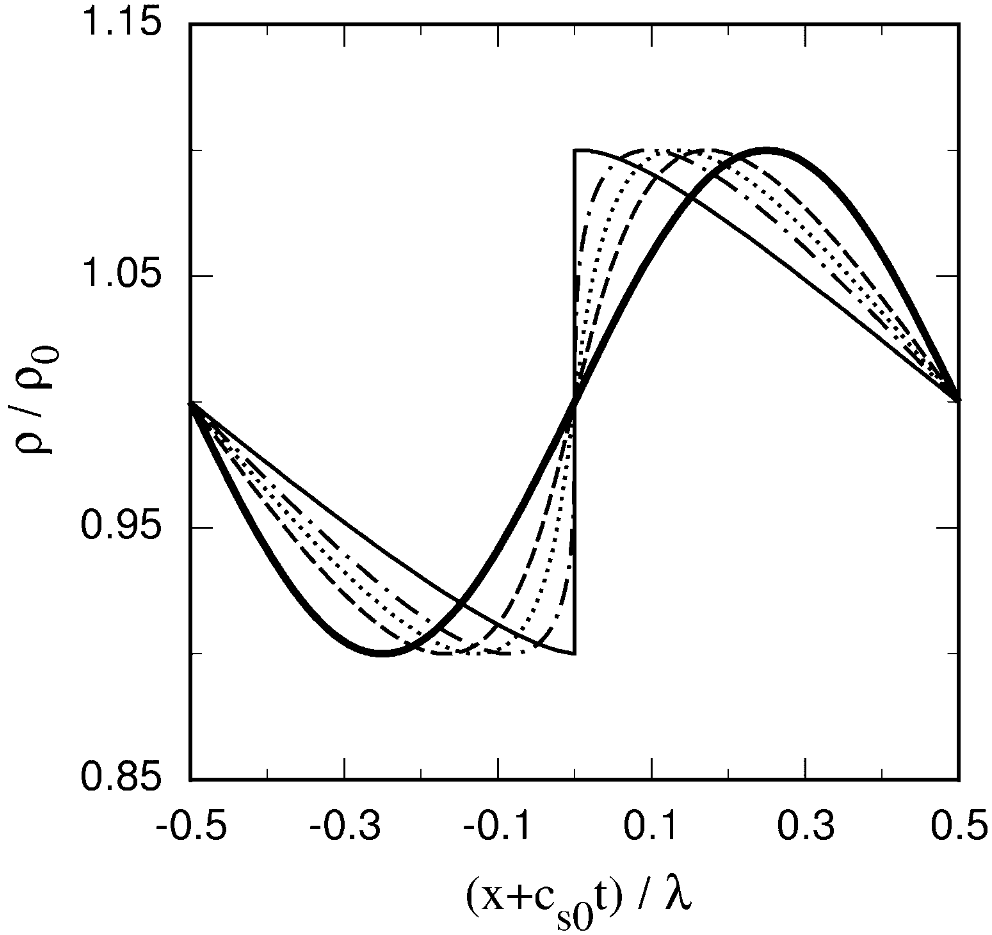

1) **Sinusoidal initial conditions.**
2) **Sine wave steepens into shock after traveling several periods.**
3) **Solution shown in moving frame of reference.**

Exact solution is available until shock forms at $t=t_b$.

Convergence rates depend on order of accuracy of subgrid-scale models.

Compressible breaking wave

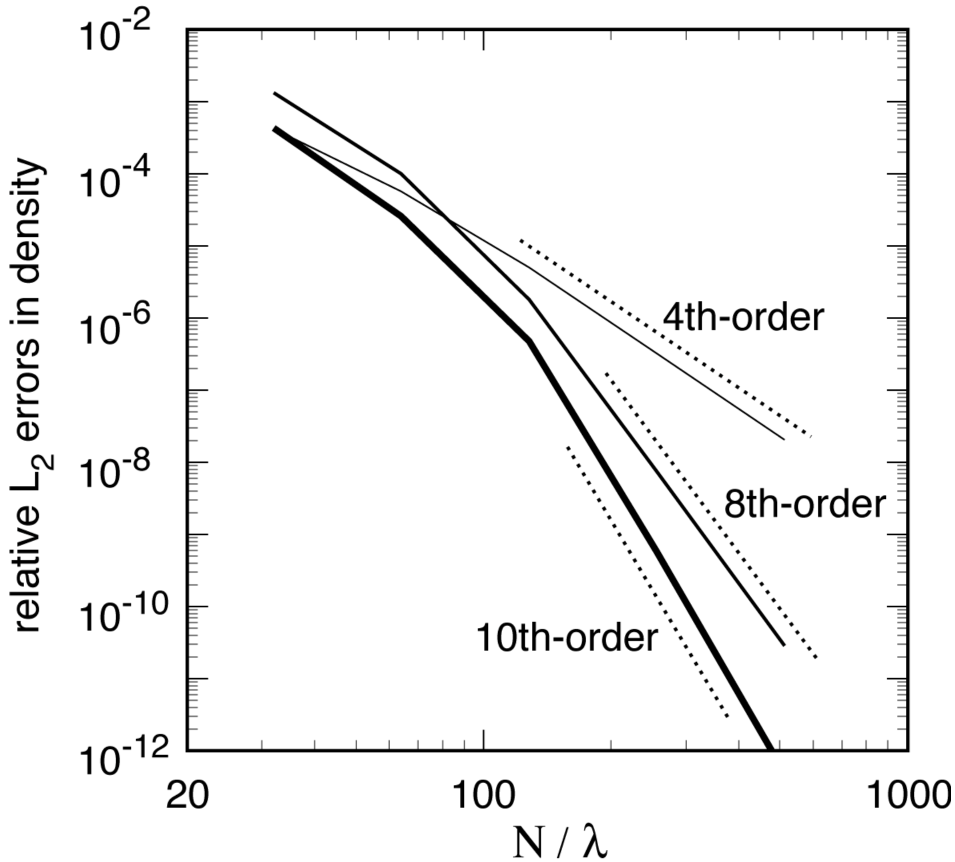

1. Sinusoidal initial conditions.
2. Sine wave steepens into shock after traveling several periods.
3. Errors shown just prior to shock formation.

1. At high CFL numbers convergence is determined by timestepping scheme.
2. At low CFL numbers convergence is determined by lesser of:
   a. r parameter in subgrid model
   b. spatial differencing scheme

Spectrum broadens as flow evolves.

Errors for compact scheme are small when flow is smooth.

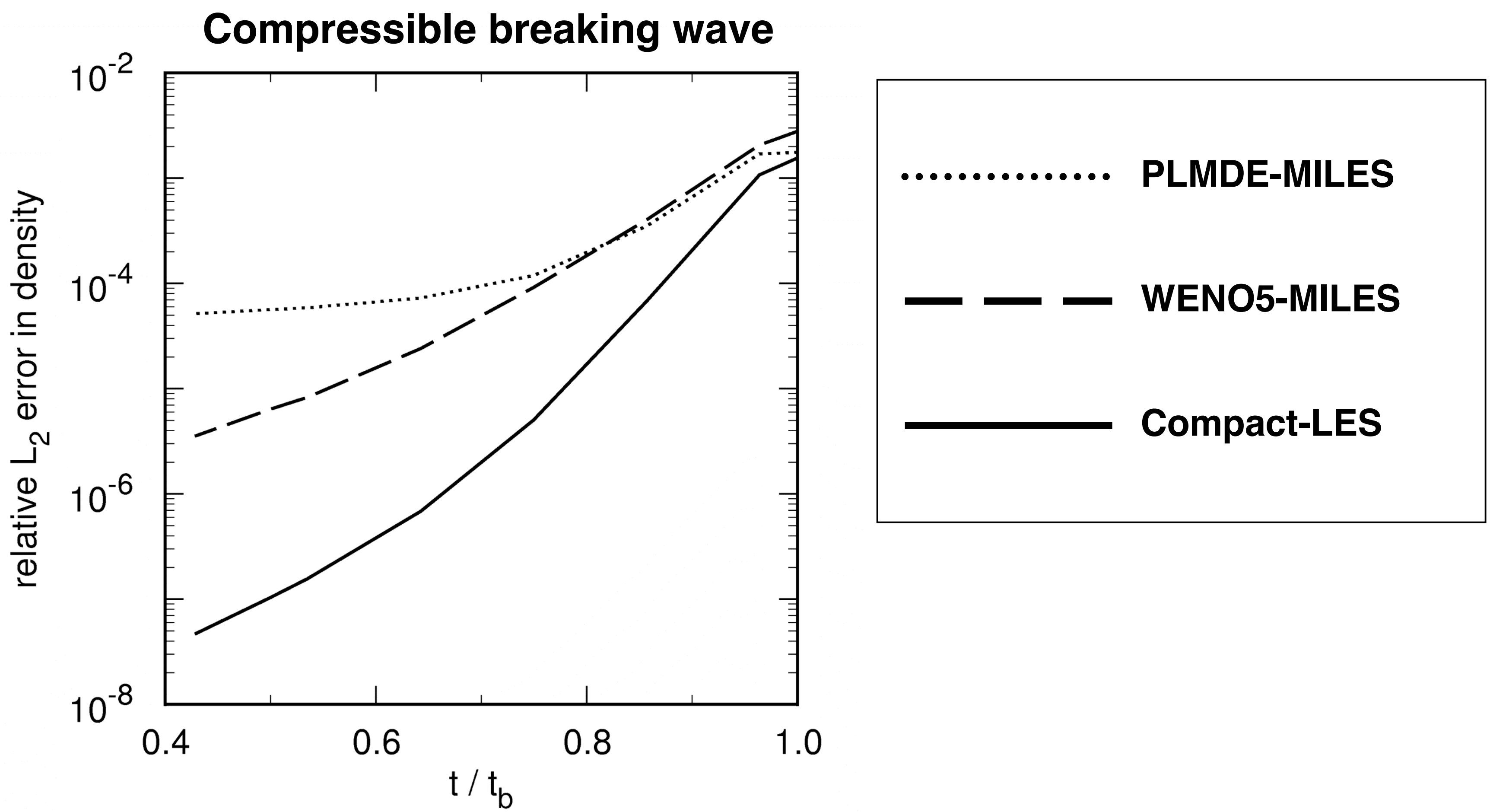

Late-time errors are due to thickness of shock.

Spectral and compact methods can capture shocks.

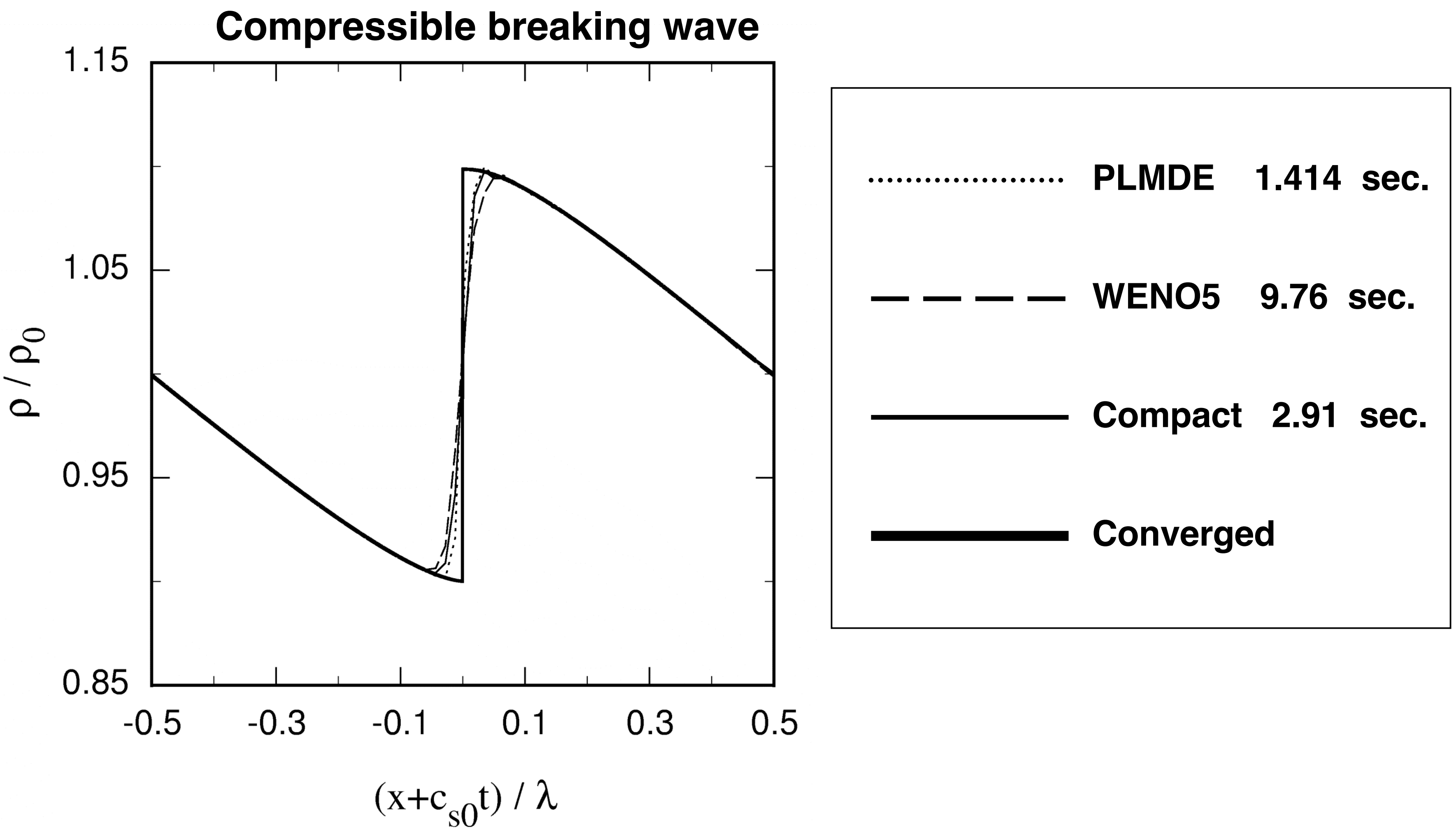

3 points in shock.

Spectral and compact methods provide superior representation of high-wavenumbers.

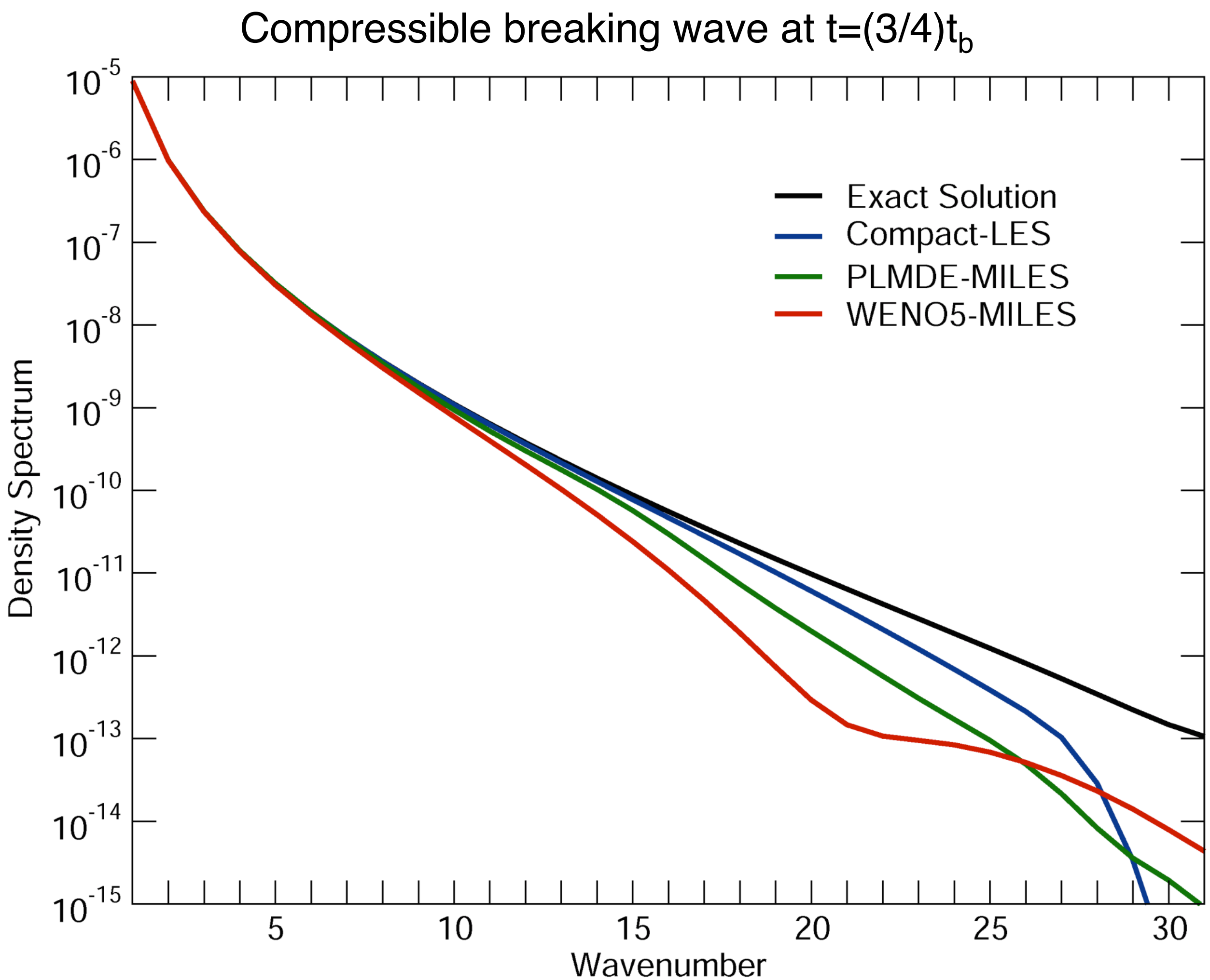

Can a deconvolution model fix the WENO spectrum?

Compact methods exhibits rapid convergence for Shu's problem.

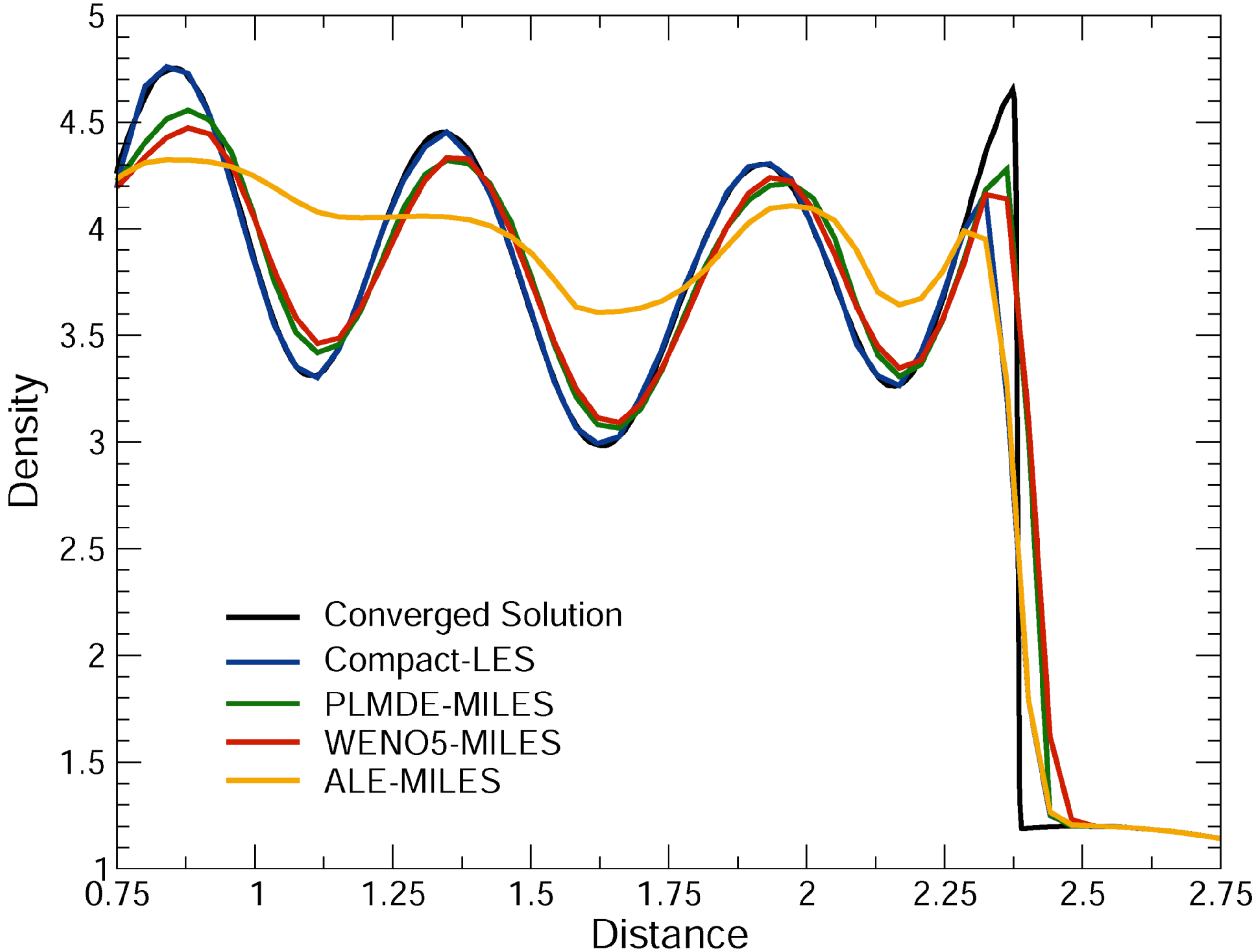

Implicit viscosity in MILES algorithms causes phase shift.

Spectral/compact methods produce superior results on the Taylor-Green vortex.

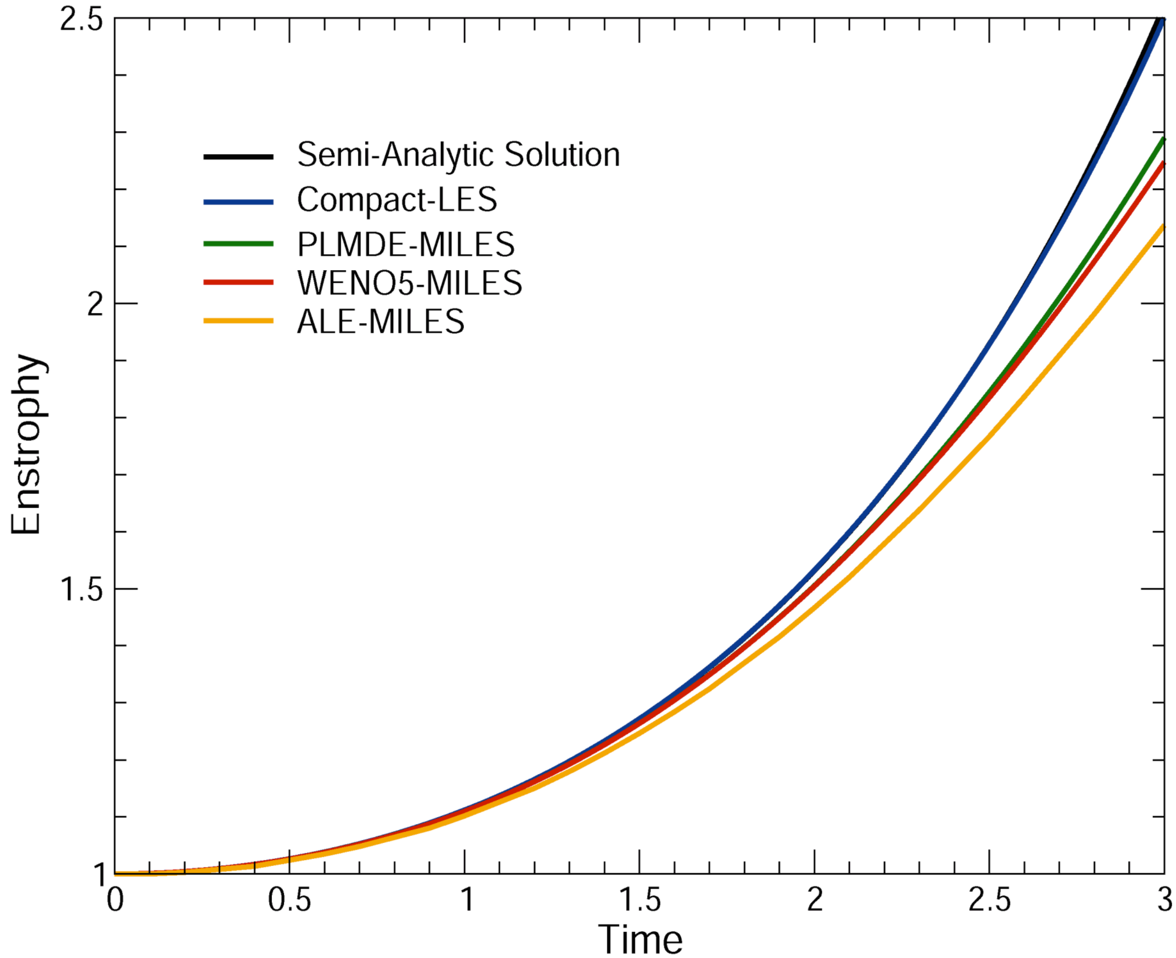

- **Energy initially at bottom wavenumber.**
- **Vortex stretches and bends.**
- **Vorticity coalesces at small scales.**
- **Energy cascades to higher wavenumbers.**

Upwinding and flux-limiting corrupt high wavenumbers.

Spectral methods with hyperviscosity perform well for decaying turbulence.

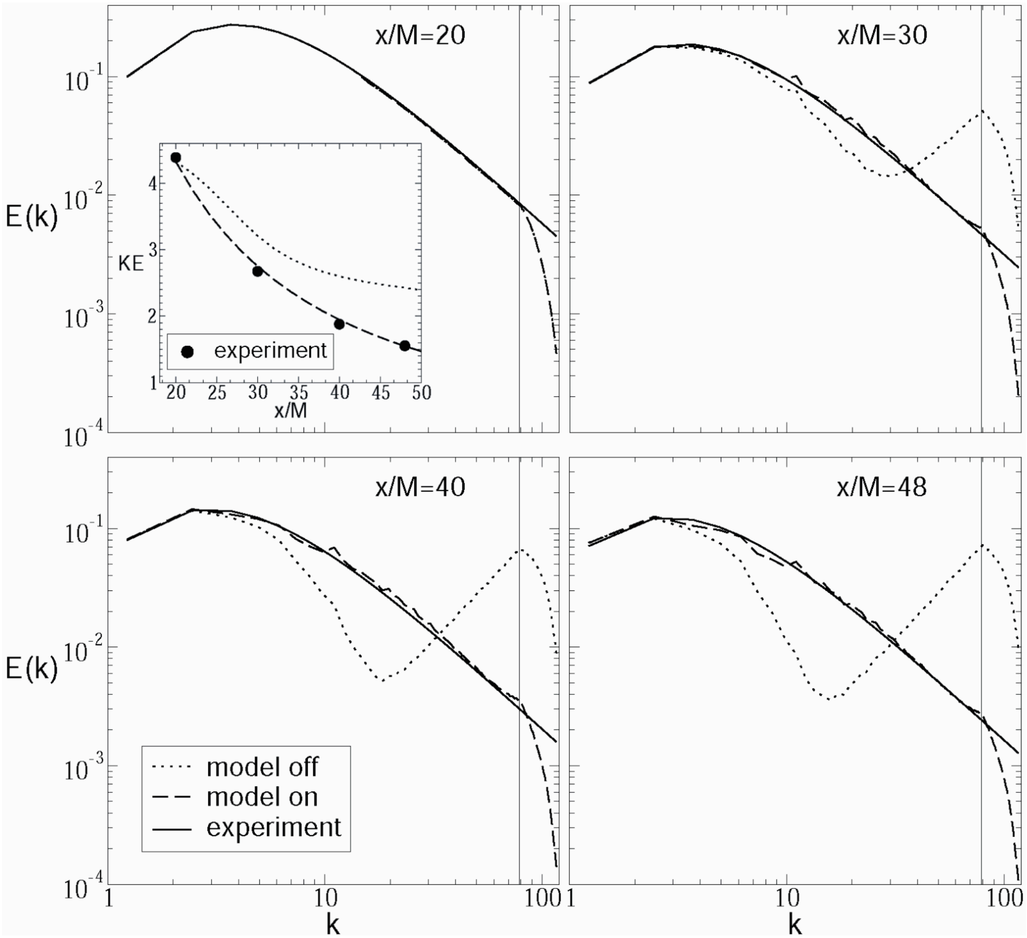

- 192^3 spectral LES
- k > 64 truncated
- matched spectrum at x/M=20
- periodic boundaries
- r = 2
- $C_\mu^r = 0.025$

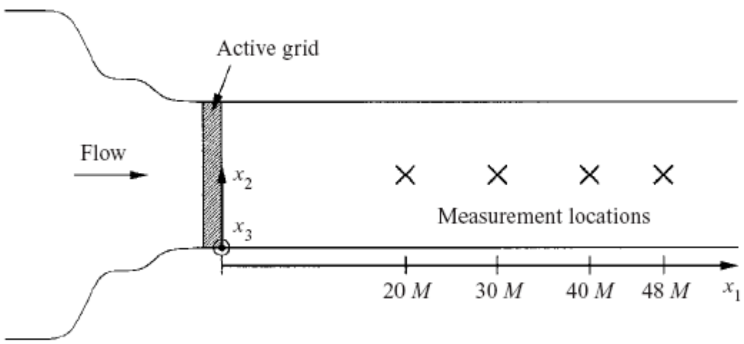

The empirical coefficient is tuned to match the energy spectrum from the grid turbulence experiment of Kang et al.

Conclusions

- TNS (Truncated Navier-Stokes) is a useful paradigm for LES.
- Spectral and compact methods can capture shocks when combined with a spectral-like bulk viscosity.
- SGS models based on high-wavenumber damping preserve convergence rates of high-order numerical methods.
- High-wavenumber SGS models allow for broader inertial range by minimizing extent of dissipation range.
- Compact-LES provides superior resolution of turbulent flows compared to MILES.

High-order LES can succeed where low-order MILES fails.